

# Ab-initio theory of metal-insulator interfaces in a finite electric field

Massimiliano Stengel<sup>1</sup> and Nicola A. Spaldin<sup>1</sup>

<sup>1</sup>Materials Department, University of California, Santa Barbara, CA 93106-5050, USA

(Dated: December 2, 2024)

We present a novel technique for calculating the dielectric response of metal/insulator heterostructures. This scheme allows, for the first time, the fully first-principles calculation of the microscopic properties of thin-film capacitors at finite bias potential. The method is general and can be readily applied to pure insulators, where it yields substantially improved accuracy compared to preexisting finite-field techniques. We demonstrate the effectiveness of our method by performing comprehensive numerical tests on a model Ag/MgO/Ag heterostructure. Future applications to the emerging field of electronic devices based on ferroelectric materials are discussed.

PACS numbers: 71.15.-m

The dielectric response of a metal-insulator interface to an applied electric field is a subject of great interest nowadays, as the ongoing miniaturization of electronic devices is reaching the atomic scale. In this regime, the properties of thin oxide films (used e.g. in nonvolatile ferroelectric memories [1] and as gate oxides in MOSFET transistors [2]) start to deviate from those predicted by macroscopic models, and cannot be disentangled from the metallic or semiconducting contact [3]. One particularly important issue related to interfacial effects is the “dielectric dead layer” [4], which plagues the performance of thin ferroelectric capacitors by substantially reducing the effective permittivity ( $\kappa$ ) of the active high- $\kappa$  material. Interface chemistry [5], finite screening length in the metal [6], or the presence of structural and point defects could each be responsible for the experimentally observed permittivity depletion, but a generally accepted explanation is still missing. In order to separate these effects and to help improve over the existing models, the electronic and ionic response of a metal-insulator heterostructure to an external bias potential must be understood at the quantum mechanical level.

First-principles calculations, especially within the framework of density functional theory, have proven to be a powerful tool in the fundamental understanding of metal-ceramic interfaces [7]. On the other hand, *ab initio* studies of interfacial dielectric properties are still in their infancy, and only *insulating* heterostructures have been successfully simulated [5] in a finite external field. Indeed, when one of the two materials is a metal (as required for the simulation of a realistic thin-film capacitor), the presence of partially filled bands at the Fermi level prevents the straightforward application of the Berry-phase technique [8], on which most finite electric field calculations have been based so far [9, 10]. In order to gain further insight into the rich domain of phenomena occurring at metal-dielectric junctions there is the clear need for a methodology that allows one to work around this obstacle.

In this work we demonstrate how this problem can be solved by using techniques and ideas borrowed from

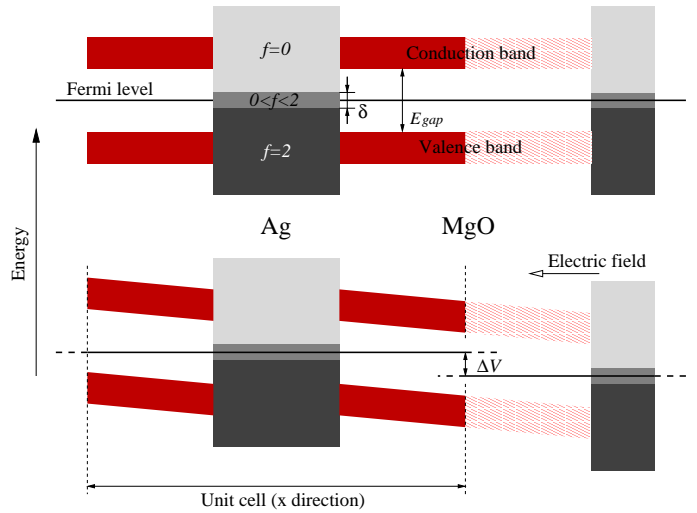


FIG. 1: Schematic representation of the projected band structure of a metal-insulator heterostructure in the absence of (top) and with (bottom) electric field. An effective bias potential  $\Delta V$  between one slab and the repeated images is obtained.

Wannier-function theory, which is an appealing alternative to the traditional Berry-phase formalism [11]. In particular, we show that the insulating nature of a capacitor under an applied bias potential is reflected at the microscopic level in the confinement of the metal-induced gap states, whose propagation in the insulator is forbidden; this property allows for a rigorous definition of the polarization and the coupling to an external field, in close analogy to purely insulating systems. We demonstrate the effectiveness of our technique using a model MgO/Ag(100) heterostructure; the simple properties of this well studied metal-ceramic interface make it an ideal test case for our method. In addition to providing a technical validation to our approach, our results indicate that MgO films retain an ideal classical behavior in the ultra-thin limit, corroborating the picture that emerged from previous investigations [12].

The coupling of a periodic system to a finite external

field  $\mathcal{E}$  is described by the electric enthalpy [10]:

$$E^{\mathcal{E}} = E_{KS} - \Omega \mathcal{E} \cdot \langle P \rangle, \quad (1)$$

where  $E_{KS}$  is the Kohn-Sham total energy,  $\Omega$  is the volume of the supercell and  $\langle P \rangle$  is the macroscopic polarization along the field axis (indicated hereafter as  $x$ ); in a parallel-plate capacitor this is always perpendicular to the electrode plane. Within periodic boundary conditions,  $\langle P \rangle$  is commonly evaluated using a Berry phase [8] or a many-body position operator [11]; these techniques, however, are incompatible with the fractional orbital occupancies which stem from the metallicity of the electrodes. As an alternative, within a single-particle theory,  $\langle P \rangle$  can be equivalently related to the centers of the Wannier functions [8] (WFs), or to “hermaphrodite” WFs [13, 14], which are maximally localized along  $x$  and Bloch-like in the electrode ( $yz$ ) plane. These are ideally suited to representing the inherently delocalized nature of electrons in the two-dimensionally conducting plates, while providing a fast spatial decay (which is crucial to an accurate definition of  $\langle P \rangle$  [15]) along the field direction ( $x$ ). To achieve a localized representation along  $x$  in practice, we divide the problem into three regimes, which are identified independently for every  $k$ -point of the surface Brillouin zone (a schematic representation is shown in Fig. 1):

- The completely empty states with zero occupation numbers are discarded from the computation, since they do not contribute to the ground state energy or charge density.
- The submanifold of fully occupied valence states (with energy eigenvalue  $\epsilon_n < E_F - \delta$  in Fig. 1) is localized separately by means of the parallel-transport algorithm [16, 17]; this operation leaves the total energy unaffected.
- The partially occupied states in the region of the Fermi level (shown in gray in Figure 1) lie in the energy gap of the dielectric; as a result they are quantum mechanically confined in the metallic slab without taking any further action, since they cannot propagate through the insulator.

The centers,  $x_n$ , of the resulting set of localized orbitals can then be obtained by using periodic sawtooth functions (details of the technique are reported in Ref. 15), and the polarization defined as:

$$\langle P \rangle = \frac{1}{\Omega} \left( \sum_n f_n x_n + \sum_I q_I X_I \right), \quad (2)$$

where  $f_n$  is the occupancy of the  $n$ -th localized orbital,  $q_I$  is the charge of the  $I$ -th pseudoatom and  $X_I$  its  $x$  coordinate; the multi-valuedness in the definition of  $x_n$  (modulus a lattice vector) is removed by imposing  $x_n \in$

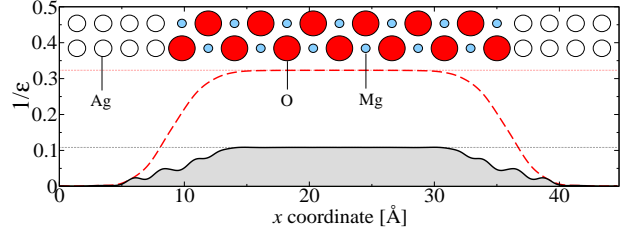


FIG. 2: High-frequency (red dashed curve) and static (black shaded curve) permittivity profiles for the Ag/MgO heterostructure. Bulk values for the permittivity are indicated as thin dotted lines. The approximate position of the atomic planes is sketched in the upper part of the figure.

$[-L/2, L/2]$ , with the origin  $x = 0$  corresponding to the center of the metallic slab and  $L$  the cell length. The contribution  $\Delta \hat{H}^{\mathcal{E}}$  to the Hamiltonian due to the electric field operator is written as a non-local, state-dependent potential  $F_n(x)$  applied to each WF,  $w_n$ , individually:

$$\Delta \hat{H}^{\mathcal{E}} = \mathcal{E} \sum_n |\hat{F}_n w_n \rangle \langle w_n|. \quad (3)$$

The  $F_n(\mathbf{r})$  are periodic sawtooth functions [27] of the form  $F_n(\mathbf{r}) = x$ , with  $x \in [x_n - L/2, x_n + L/2]$ , i.e.  $F_n(0, y, z) = 0$  for every  $n$ , and is discontinuous in a point located far from the center  $x_n$ , where the corresponding orbital has vanishing importance [28]. We note that the average value of  $F_n(x)$  over the cell is irrelevant for a purely insulating system, but is crucial when a metallic electrode is present. It can be easily verified that our choice respects the correct limit in the case of an isolated metallic slab in vacuum, where the field operator becomes *local*. This also means that, when a center  $x_n$  crosses the point  $x = L/2$  (the center of the insulating slab), the corresponding polarizing potential  $\mathcal{E} F_n(x)$  undergoes a discontinuous, rigid jump of magnitude  $\Delta V = \pm \mathcal{E} L$ . For a sufficiently thick insulating layer, and as long as  $\Delta V$  is small enough not to bring valence or conduction states into the partially occupied region close to the Fermi level, this jump leaves the system unaffected apart from a trivial shift of the total energy by a quantum of polarization (the discontinuity can also be effectively smoothed by smearing the  $F_n$  with Gaussian functions). Interestingly, the large-field Zener instability reported for purely insulating bulk materials [9, 10] translates here to a *Schottky-tunneling* instability that has to be avoided by careful analysis of the band alignment. We note that insulating heterostructures or bulk systems are limiting cases of our approach, and therefore our method can be considered a generalization of existing finite field techniques [29]. In particular, the theory of local permittivity that was originally developed for purely insulating interfaces [14] is directly applicable, and can be readily generalized as follows to obtain the first-principles capacitance density per unit area,  $\mathcal{C}$ . We start from the usual textbook definition

of the capacitance density,

$$\mathcal{C} = \frac{\sigma}{\Delta V}, \quad (4)$$

with  $\Delta V = \mathcal{E}L$  the potential drop between the electrodes, and  $\sigma$  the surface density of the *free* charge stored in the device. From classical electrostatics, the free charge is equal to the value of the induced polarization deep inside the electrode, where the applied field is completely screened. In our geometry this occurs in the center ( $x = 0$ ) of the metallic slab, and Eq. 4 reduces to

$$\mathcal{C} = \frac{\Delta \bar{P}(x = 0)}{\mathcal{E}L} \quad (5)$$

where  $\Delta \bar{P}(x)$  is the planar- and macroscopically-averaged [18] induced polarization. Finally,  $\Delta \bar{P}(0)$  can be extracted from the relationship, derived in Ref. [14], between the local permittivity,  $\bar{\epsilon}(x)$ , and induced polarization, and the corresponding globally averaged quantities  $\langle \epsilon \rangle$  and  $\langle \Delta P \rangle$ :

$$\left(1 - \frac{1}{\bar{\epsilon}(x)}\right) = \left(1 - \frac{1}{\langle \epsilon \rangle}\right) \frac{\Delta \bar{P}(x)}{\langle \Delta P \rangle}. \quad (6)$$

Since deep in the metal  $\bar{\epsilon}(x)$  diverges [i.e.  $1/\bar{\epsilon}(0) = 0$ ], Eq. 6 reduces simply to  $\Delta \bar{P}(x = 0) = \langle \Delta P \rangle + \mathcal{E}/(4\pi)$ , and Eq. 4 reduces to

$$\mathcal{C} = \frac{\langle \epsilon \rangle}{4\pi L}, \quad (7)$$

where  $\langle \epsilon \rangle = 4\pi \langle \Delta P \rangle / \mathcal{E} + 1$  is the overall dielectric constant of the supercell, and  $\langle \Delta P \rangle$  is the polarization induced by the field  $\mathcal{E}$ . We use equation 7 to obtain the capacitance values in the examples below.

We demonstrate the effectiveness of our scheme by presenting results for a model  $[\text{Ag}(100)]_n / [\text{MgO}(100)]_m$  heterostructure [30], with the thicknesses of the Ag and MgO slabs set to  $n = 9$  and  $m = 13$  atomic layers, respectively, and the O atoms placed in the atop position. The out-of-plane atomic positions and cell parameter were relaxed in zero field until the maximum force was lower than 0.05 meV/Å, and the spacing  $t_0$  between the central MgO layers was within 0.2% of the bulk equilibrium value. We then imposed an external field of 51.4 V/μm and relaxed the electrons to the ground state while keeping the ions fixed. The resulting high-frequency permittivity profile is shown as a thick dashed curve in Fig. 2. On the metal side of the interface the inverse permittivity drops quickly to zero, as expected, while it is very close to the bulk MgO value [31] after only three atomic layers on the insulator side. The calculated value in the middle of the MgO slab is  $\bar{\epsilon}^\infty(L/2) = 3.095$ , which is within 0.03% of the bulk value,  $\epsilon_{\text{bulk}}^\infty = 3.094$ . This level of accuracy is impressive, especially when compared to previous calculations of insulating heterostructures based on the Berry-phase approach, where errors introduced solely by

the finite field formalism were estimated to be of the order of 10% [14]. The ionic forces  $f_I$  extracted from the finite-field ground state calculation provide also the Born effective charges  $Z_I^* = f_I/\mathcal{E}$  of all atoms at once [10] [32].

Once the  $Z_I^*$  are defined, the ionic contribution to the static polarization can be either evaluated in the linear (zero field) approximation with standard linear-response techniques [19], or non-perturbatively, by performing a direct relaxation in a finite external field [10]. First we computed the symmetry-restricted force matrix of the system by the finite-difference method in zero field using small displacements of 0.0004 Å along  $x$ . The variation of the *local* polarization upon atomic displacements,  $\delta \bar{P}(x, \{R_I\})/\delta R_I$ , was also simultaneously extracted for each degree of freedom and used, together with the force matrix and the Born effective charges, to construct the static permittivity profile,  $\bar{\epsilon}^0(x)$ , which is shown as a thick solid curve in Fig. 2. The behavior of the static and high frequency permittivities are similar, the only relevant difference being their magnitudes in the middle of the insulating slab, with  $\bar{\epsilon}^0(L/2)$  converging to a value of 9.227 ( $\epsilon_{\text{bulk}}^0 = 9.229$ ). Next, we performed a direct relaxation of the atomic positions in an external bias  $\Delta V = 1.15$  V, which corresponds roughly to a self-consistent field of 400 V/μm throughout the dielectric; the resulting average permittivity was within 0.05% of the zero field linear response value, indicating as expected the absence of anharmonic effects in this field regime within numerical accuracy.

Having assessed the reliability of our technique, and obtained accurate profiles, we next extracted the static and high-frequency values of the capacitance, obtaining  $\mathcal{C}^0 = 31.2 \text{ fF}/\mu\text{m}^2$  and  $\mathcal{C}^\infty = 10.3 \text{ fF}/\mu\text{m}^2$  respectively. These values are respectively 3.1% and 1.2% higher than the classical estimates based only on the knowledge of the bulk permittivity and of the thickness of the film:

$$\mathcal{C}_{\text{classical}}^{(0,\infty)} = \frac{\epsilon_{\text{bulk}}^{(0,\infty)}}{4\pi m t_0} \quad (8)$$

The close similarity between  $\mathcal{C}$  and  $\mathcal{C}_{\text{classical}}$  indicates that the influence of the metal on the dielectric properties of the MgO film is very small. Previous investigations of ultrathin MgO films deposited on Ag have already evidenced a surprisingly fast recovery of the bulk oxide properties as a function of film thickness [12]; here we see that this result also holds for the *dielectric* properties of MgO films, which show a nearly ideal classical behaviour down to the nanometer scale.

Finally, to demonstrate the suitability of our method for calculating finite-temperature effects, we performed a microcanonical molecular dynamics run [20] by starting from the centrosymmetric zero-field equilibrium structure and letting the atoms evolve along the  $x$  axis under an external bias of  $\Delta V = 1.15$  V. The evolution of the potential energy  $E^\mathcal{E}$ , of the “physical” constant of

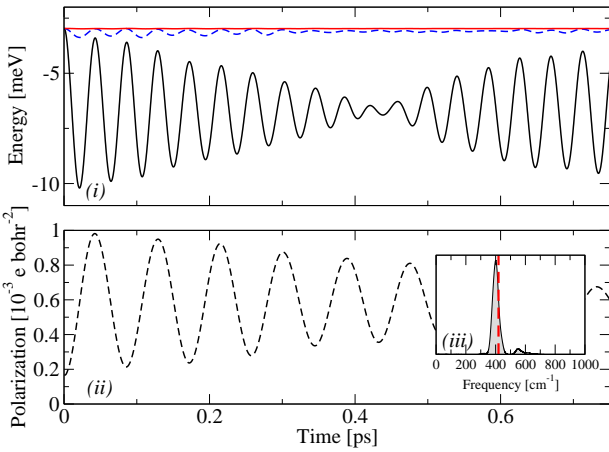


FIG. 3: (i) Energy conservation during molecular dynamics in an external bias of 1.15 V. Represented are  $E^\varepsilon$  (black solid),  $E^\varepsilon + K_{ion}$  (blue dashed) and  $E^\varepsilon + K_{ion} + K_{fake}$  (red solid). The zero of the energy scale is set at the ground state total energy in zero field. (ii) Polarization,  $\langle P \rangle$ , as a function of time. (iii) Frequency-resolved dipolar activity of the system (black shaded curve); zone-center transverse optical phonon frequency of bulk MgO is also shown (red dashed line).

motion  $E^\varepsilon + K_{ion}$  and of the approximate “mathematical” constant of motion  $E^\varepsilon + K_{ion} + K_{fake}$  ( $K_{ion}$  is the ionic kinetic energy, while  $K_{fake}$  is the fictitious electronic kinetic energy [21]) are shown in the upper panel of Fig. 3. The quality of the energy conservation is excellent; the curve has no appreciable drift, even when enlarging the vertical scale by three orders of magnitude. In the lower panel we show the evolution of  $\langle P \rangle$ , which undergoes quasiperiodic oscillations of approximate frequency  $390 \text{ cm}^{-1}$ . To link the molecular dynamics run to the lattice-dynamical properties of the system extracted from the force matrix, in the inset we show the phonon spectrum broadened by a Gaussian width of  $20 \text{ cm}^{-1}$  and weighted by the dipolar activity of the mode,  $[Z^*(\omega)]^2$ , where  $Z^*(\omega)$  is the mode effective charge [22]. The dominant peak, centered at  $400 \text{ cm}^{-1}$ , closely corresponds to the main oscillation period of the polarization  $\langle P \rangle$  during the dynamics; the frequency of the zone-center transverse optical mode of bulk MgO ( $420 \text{ cm}^{-1}$ ) is indicated as a thick dashed line.

In summary, we have developed a first-principles method for calculating the response of hybrid metal/insulator structures to an electric field, and have demonstrated its applicability by calculating the local permittivity and capacitance of a model thin-film capacitor. The method is also appropriate for insulating materials at finite bias, where it provides greater accuracy than conventional techniques, in both the linear and anharmonic regimes with respect to field and temperature; this is crucial in the simulation of ferroelectric devices, where anharmonic effects are an essential physical ingredient for a realistic description [22].

The generality of the technique is evidenced by the high quality of overall energy conservation in molecular dynamics, which suggests fascinating applications to phenomena occurring at liquid/electrode interfaces, e.g. the recently observed freezing of interfacial water under electric fields [23].

This work was supported by the National Science Foundation’s Division of Materials Research through the Information Technology Research program, grant number DMR-0312407, and made use of MRL Central Facilities supported by the National Science Foundation under award No. DMR-0080034

- [1] C. H. Ahn, K. M. Rabe, and J.-M. Triscone, *Science* **303**, 488 (2004).
- [2] K. Eisenbeiser, J. M. Finder, Z. Yu, J. Ramdani, J. A. Curless, J. A. Hallmark, R. Droopad, W. J. Ooms, L. Salem, S. Bradshaw, et al., *Appl. Phys. Lett.* **76**, 1324 (2000).
- [3] M. Dawber, K. M. Rabe, and J. F. Scott, *cond-mat/0503372* (2005).
- [4] C. Zhou and D. M. Newns, *J. Appl. Phys.* **82**, 3081 (1997).
- [5] F. Giustino, P. Umari, and A. Pasquarello, *Phys. Rev. Lett.* **91**, 267601 (2003).
- [6] J. Junquera and P. Ghosez, *Nature* **422**, 506 (2003).
- [7] M. W. Finnis, *J. Phys.: Condens. Matter* **8**, 5811 (1996).
- [8] R. D. King-Smith and D. Vanderbilt, *Phys. Rev. B* **47**, R1651 (1993).
- [9] I. Souza, J. Íñiguez, and D. Vanderbilt, *Phys. Rev. Lett.* **89**, 117602 (2002).
- [10] P. Umari and A. Pasquarello, *Phys. Rev. Lett.* **89**, 157602 (2002).
- [11] R. Resta, *J. Phys.: Condens. Matter* **14**, R625 (2002).
- [12] S. Schintke, S. Messerli, M. Pivetta, F. Patthey, L. Libioulle, M. Stengel, A. D. Vita, and W. D. Schneider, *Phys. Rev. Lett.* **87**, 276801 (2001).
- [13] C. Sgiarollo, M. Peressi, and R. Resta, *PRB* **64**, 115202 (2001).
- [14] F. Giustino and A. Pasquarello, *Phys. Rev. B* **71**, 144104 (2005).
- [15] M. Stengel and N. A. Spaldin, *cond-mat/0506389* (2005).
- [16] N. Marzari and D. Vanderbilt, *Phys. Rev. B* **56**, 12847 (1997).
- [17] Ü. V. Waghmare, N. A. Spaldin, H. C. Kandpal, and R. Seshadri, *Phys. Rev. B* **67**, 125111 (2003).
- [18] A. Baldereschi, S. Baroni, and R. Resta, *Phys. Rev. Lett.* **61**, 734 (1988).
- [19] S. Baroni, S. de Gironcoli, and A. D. Corso, *Rev. Mod. Phys.* **73**, 515 (2001).
- [20] J. Vandevondele and A. De Vita, *Phys. Rev. B* **60**, 13241 (1999).
- [21] R. Car and M. Parrinello, *Phys. Rev. Lett.* (1985).
- [22] A. Antons, J. B. Neaton, K. M. Rabe, and D. Vanderbilt, *Phys. Rev. B* **71**, 024102 (2005).
- [23] E.-M. Choi, Y.-H. Yoon, S. Lee, and H. Kang, *Phys. Rev. Lett.* **95**, 187402 (2005).
- [24] J. P. Perdew and Y. Wang, *Phys. Rev. B* **45**, 13244 (1992).

- [25] P. E. Blöchl, Phys. Rev. B **50**, 17953 (1994).
- [26] F. Giustino and A. Pasquarello, Phys. Rev. Lett. **95**, 187402 (2005).
- [27] The  $F_n(\mathbf{r})$  are constructed in reciprocal space in order to avoid Fourier aliasing errors and preserve analytical gradients.
- [28]  $\Delta\hat{H}'$  has in general a small anti-Hermitian part that we remove by introducing a correction term of the form

$$\Delta\hat{H}'|w_i\rangle = \frac{\mathcal{E}}{2} \sum_j |w_j\rangle\langle w_j|(F_j - F_i)|w_i\rangle.$$

This term goes exponentially to zero with increasing insulator thickness, and vanishes if each Wannier-like state is strictly localized in  $x \in [x_n - L/4, x_n + L/4]$ . With this correction, we could always achieve optimal convergence to the electronic ground state.

- [29] Due to the better convergence properties as a function of  $L$  [15] our method is also expected to be substantially more accurate than the customary Berry-phase-based approach for a given choice of geometry and  $k$ -point sampling.

- [30] Our calculations were performed within the local density approximation [24] and the PAW method [25], with a plane wave cutoff of 40 Ry, a Gaussian smearing of 0.2 eV for the orbital occupancies and 10 special  $k$ -points in the surface Brillouin zone. The in-plane lattice constant was fixed to the calculated equilibrium value of bulk MgO ( $a_0=7.86$  a.u.). For all electronic and ionic relaxations we used an extension of the Car and Parrinello [21] method to metallic systems.
- [31] The bulk calculations were performed on a tetragonal 8-layer non-primitive supercell with the same in-plane lattice parameter and  $k$ -point sampling as the interface system. The out-of-plane spacing was set to  $t_0$ .
- [32] In the middle of the MgO film,  $Z_O^*$  and  $Z_{Mg}^*$  have opposite values within numerical accuracy, but they differ from the bulk  $|Z_{bulk}^*| = 1.95$  by a factor of  $\langle\epsilon^\infty\rangle/\epsilon_{bulk}^\infty$  [26]; taking into account this factor, the matching is better than 0.05%.